applied sciences

MDPI

Article

Energy Management Strategy Based on V2X Communications and Road Information for a Connected PHEV and Its Evaluation Using an IDHIL Simulator

Seongmin Ha [1,2] and Hyeongcheol Lee [3,*]

[1] Department of Electrical Engineering, Hanyang University, 222, Wangsimni-ro, Seongdong-gu, Seoul 04763, Republic of Korea; haha4100@hanyang.ac.kr
[2] Strategic Planning Division, Korea Intelligent Automotive Parts Promotion Institute, 201, Gukgasandanseo-ro, Guji-myeon, Dalseong-gun, Daegu 43011, Republic of Korea
[3] Department of Electrical and Biomedical Engineering, Hanyang University, 222, Wangsimni-ro, Seongdong-gu, Seoul 04763, Republic of Korea
* Correspondence: hclee@hanyang.ac.kr; Tel.: +82-2-2220-1685

Abstract: Conventional energy management strategies (EMSs) of hybrid electric vehicles (HEVs) only utilize in-vehicle information, such as an acceleration pedal, velocity, acceleration, engine RPM, state of charge (SOC), and radar. This paper presents a new EMS using out-vehicle information obtained by vehicle to everything (V2X) communication. The new EMS integrates cooperative eco-driving (CED) guidance and an adaptive equivalent consumption minimum strategy (A-ECMS) based on V2X communication information and road information. CED provides a guide signal and a guide speed to the driver. It guides pedal behavior in terms of coasting driving, acceleration and deceleration, and target speed. A-ECMSs calculate the target SOC based on the simplified road information of the planned route and reflects it in the equivalent factor. An integrated driving hardware-in-the-loop (IDHIL) simulator is also built to prove the new EMS by integrating a V2X communication device, a VANET simulator, and a vehicle simulator. The IDHIL test results demonstrate the validity and performance of the proposed EMS in a V2X communication environment.

Keywords: energy management strategy (EMS); cooperative eco-driving (CED); vehicle to everything (V2X) communication; equivalent consumption minimum strategy (ECMS); connected plug-in hybrid electric vehicle (PHEV); integrated driving hardware-in-the-loop (IDHIL) simulator

Citation: Ha, S.; Lee, H. Energy Management Strategy Based on V2X Communications and Road Information for a Connected PHEV and Its Evaluation Using an IDHIL Simulator. *Appl. Sci.* **2023**, *13*, 9208. https://doi.org/10.3390/app13169208

Academic Editors: Fei Hui, Daxin Tian and Wei Shangguan

Received: 20 July 2023
Revised: 9 August 2023
Accepted: 10 August 2023
Published: 13 August 2023

1. Introduction

Due to global environmental issues, the number of regulations focused on the automotive industry are steadily increasing. The U.S. Corporate Average Fuel Economy (CAFE) standard aims to improve fuel economy by an average of about 5% per year from 2020 to 2025 and achieve an average fleet fuel economy of 46.7 mpg. The EU adopted regulation (EU) 2019/631, which sets targets to reduce CO_2 emissions by 15% by 2025 and 37.5% by 2030 [1].

Among the solutions to environmental regulations are hybrid electric vehicles (HEVs) and plug-in hybrid electric vehicles (PHEVs). Various approaches have been proposed as energy management strategies (EMSs) to improve the fuel economy of (P)HEVs [2–7]. Typical approaches include optimization-based solutions that determine the power distribution between the engine and the motor. These include offline optimization algorithms such as linear programming and dynamic programming and online optimization algorithms such as Pontryagin's minimum principle (PMP), model predictive control (MPC), and the equivalent consumption minimization strategy (ECMS) [8]. In addition, with the help of artificial intelligence, learning-based EMSs using machine learning and reinforcement learning techniques have been proposed. Yan et al. [9] proposed a multi-objective EMS based

on deep reinforcement learning, which showed improvements from three perspectives: training effort, fuel economy, and battery degradation suppression.

The recent attention of the connected and automated vehicle (CAV) industry has led to the development of intelligent transportation system (ITS) technologies. This is expanding the possibilities of improving the EMS performance of connected (P)HEVs using vehicle to everything (V2X) communication [10]. In an effort to obtain high fuel economy, it has been identified that the performance of EMSs can be improved by utilizing various information outside the vehicle, such as road information and traffic information. Chen Zhang et al. [11] show that fuel economy is improved by considering the slope of the planned driving route through a terrain preview. Zheng et al. [12] proposed an EMS that uses traffic preview information to improve fuel economy by optimizing speed profiles and minimizing fuel consumption. Hofstetter et al. [13] proposed an EMS that utilizes forward driving path information using radar sensors. Ubiergo et al. [14] introduced an eco-driving strategy that considers traffic conditions and traffic lights using V2I communication. They compared the results for fuel economy improvement and waiting time according to market penetration rate (MPR), congestion, vehicle following model, etc.

Existing EMSs have mainly presented approaches in fixed driving cycles, such as FTP-75 and HWFET [15–18]. Recently, EMSs for connected (P)HEVs mostly derive speed and/or SOC profiles based on external information and perform optimal power distribution based on them. Guo et al. in [19] utilize traffic light timetables to optimize speed, and from this, power distribution and gear shift schedules are determined using MPC. Heppeler et al. [20] used data from navigation to compute a predictive SOC trajectory for the long horizon. This SOC trajectory was then used to optimize the combined vehicle speed and SOC for the short horizon. Qi et al. [21] proposed a connected eco-driving assistance system to optimize the operation of PHEVs by integrating powertrain and ITS technologies. Predicting a vehicle's speed based on upcoming information can reflect the changing driving environment in real time, thus improving the potential for actual vehicle fuel economy. However, connected vehicles are currently difficult to evaluate on the road. This is because there are only a limited number of locations and vehicles with ITS infrastructure and equipment. In our previous work, we developed an integrated driving hardware-in-the-loop (IDHIL) simulator equipped with real V2X communication devices [22]. This simulator integrates a vehicular ad hoc network (VANET) simulator, a V2X communication device, and a vehicle simulator (vehicle model, virtual road, neighboring vehicles, traffic signals, etc.). It can be used to simulate a virtual environment for EMS development and the evaluation of connected (P)HEVs.

In this paper, we present an EMS for PHEVs using road information and V2X communication information and evaluate it using the IDHIL simulator. The proposed EMS consists of cooperative eco-driving (CED) and adaptive ECMSs (A-ECMSs). CED utilizes road information (curvature, slope, distance, limit speed) and V2X communication information (traffic light, neighboring vehicles). The road information is simplified by dividing the entire road into several parts in advance. Using this information, speed and coasting timing are calculated and provided to the driver through visual guidance. CED guidance provides the driver with instructions to guide the target speed and pedal behavior (acceleration, deceleration, and coasting driving). The A-ECMS utilizes road information to approximate battery usage for the upcoming segment to determine the target SOC. This is reflected in the equivalent factor (EF) to calculate the optimal power distribution ratio.

This paper is organized as follows. Section 2 describes the IDHIL simulator and its improvements and additions over previous work. Section 3 describes the EMS, including CED guidance and the A-ECMS. Section 4 shows the results of the IDHIL simulation test. Section 5 discusses the results and mentions future work.

2. Integrated Driving Hardware-in-the-Loop (IDHIL) Simulator

The IDHIL simulator was organized as shown in Figure 1. It is a real-time co-simulation environment that integrates a VANET simulator, vehicle model, traffic scenario,

driving controller (wheel, accelerator/brake pedals), HIL simulator, Micro AutoBox, etc. In addition, a V2X communication device (Cohda wireless MK5) was used to make it similar to the real communication environment.

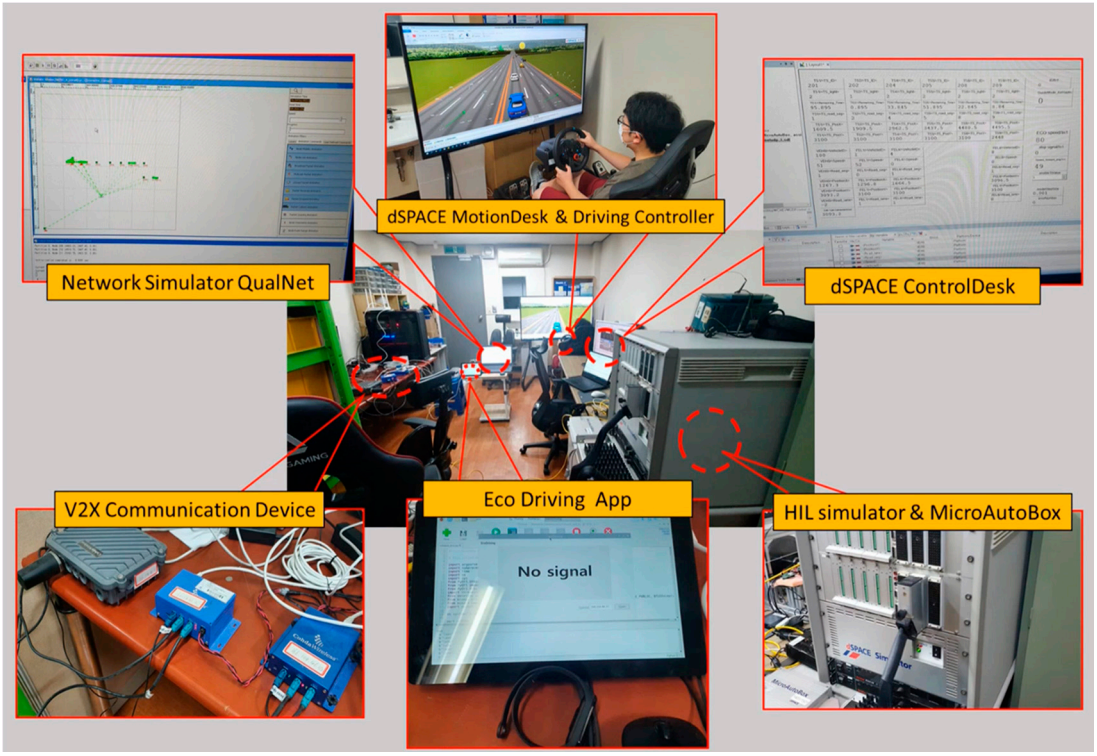

Figure 1. IDHIL simulator test environment.

2.1. Target Vehicle

The target vehicle of this study is a parallel PHEV of the transmission-mounted electric drive (TMED) type with the structure shown in Figure 2, where FD represents final drive, TM represents transmission, MG1 represents traction motor, ENG represents engine, MG2 represents belt-driven starter and generator (BSG), and BAT represents high-voltage battery.

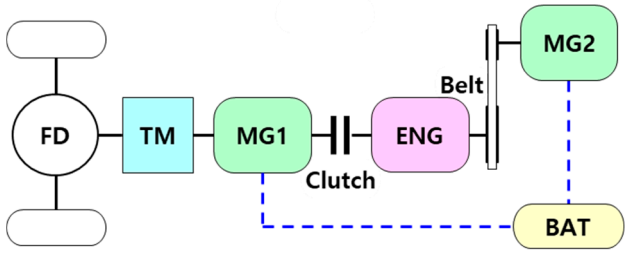

Figure 2. Configuration of TMED-type PHEV.

The vehicle model was implemented in a MATLAB/Simulink environment using dSPACE ASM traffic, as shown in Figure 3. Soft ECU blocks contained controllers for vehicle components (engine, transmission, power steering, brake) and some functions (start button, ACC, etc.). The engine block consists of the gasoline engine basic model and the fuel consumption calculation model. The drivetrain block consists of the crankshaft, clutch, shaft, transmission, and final drive models. The vehicle dynamics block consists of the tire, aerodynamics, brake, suspension, steering, and vehicle movement models. The environment block consists of the maneuver, driver, road, and traffic models. The electric system block contains models of MG1, MG2, and a battery and controller.

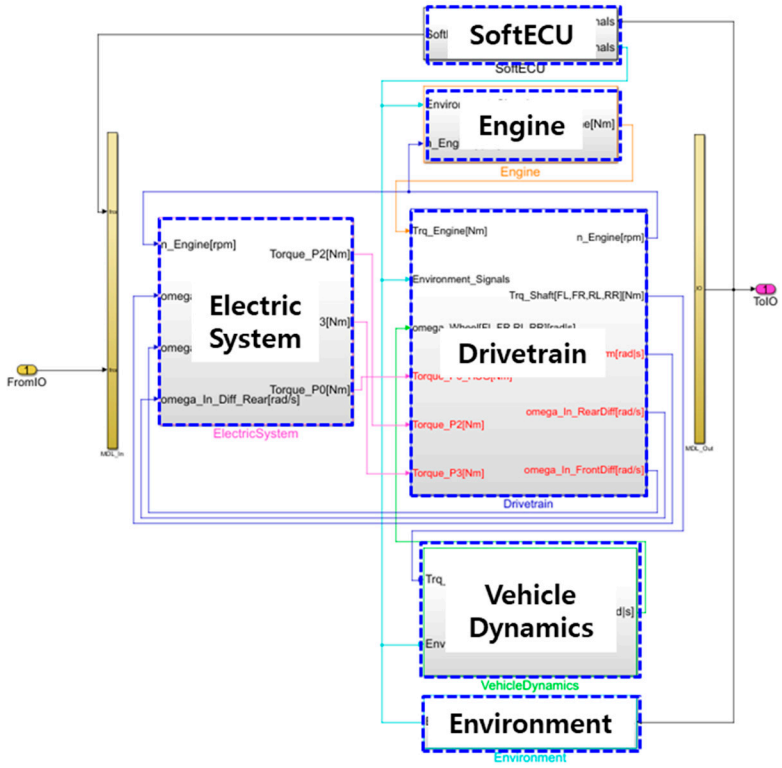

Figure 3. Vehicle model based on MATLAB/Simulink with the dSPACE ASM.

The main vehicle parameters are shown in Table 1, and the performance maps of the engine and motors are shown in Figure 4, where (a) shows the brake-specific fuel consumption (BSFC) map, maximum torque, and optimal operation line (OOL) of the engine, (b) shows the max/min torque and efficiency of MG1, and (c) shows the max/min torque and efficiency map of MG2.

Table 1. Vehicle parameters.

Parameters	Values
Vehicle mass	1725 [kg]
Engine max. power	108 [kW]
Engine max. torque	180 [Nm]
MG1 max. power	50 [kW]
MG1 max. torque	205 [Nm]
MG1 base RPM	2330 [RPM]
MG2 max. power	8.5 [kW]
MG2 max. torque	43.2 [Nm]
MG2 base RPM	1870 [RPM]
Battery voltage	360 [V]
Battery capacity	31.9 [Ah]

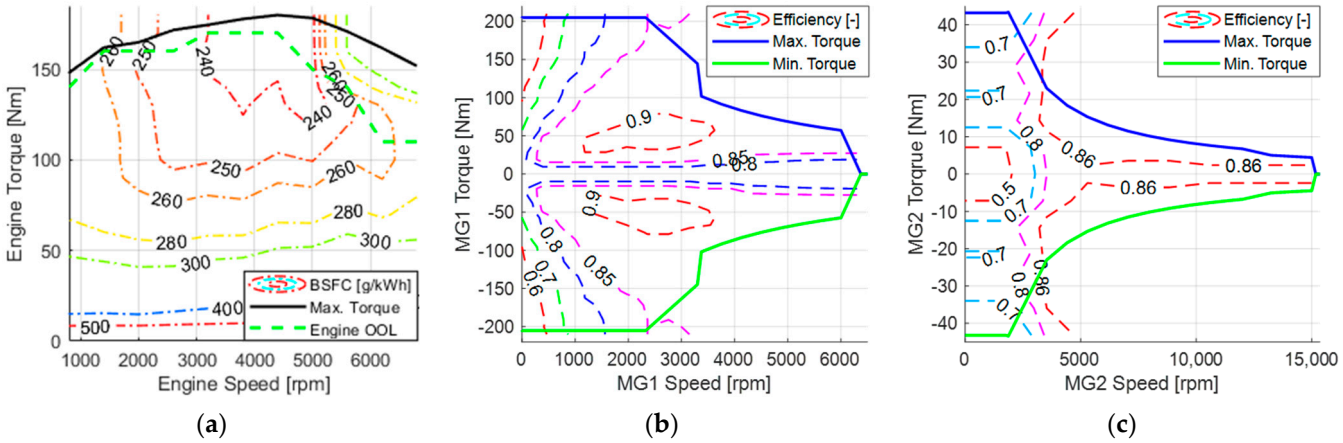

(**a**) (**b**) (**c**)

Figure 4. Performance maps: (**a**) engine; (**b**) MG1; (**c**) MG2.

2.2. Implementation of Vitual Roads for Simulation

Virtual roads were built using dSPACE ModelDesk based on the measured data of real roads, as shown in Figure 5. GNSS/INS equipment (OXTS RT3100) was used to measure the real roads, including urban roads and motorways. To create roads using ModelDesk, it is necessary to quantify and simplify measured road information. We separated roads based on slope, traffic light locations, and intersections. Each segmented road is represented as a road segment, and this information is used directly by the EMS. Road segment information consists of length, slope angle, curvature, and limit speed.

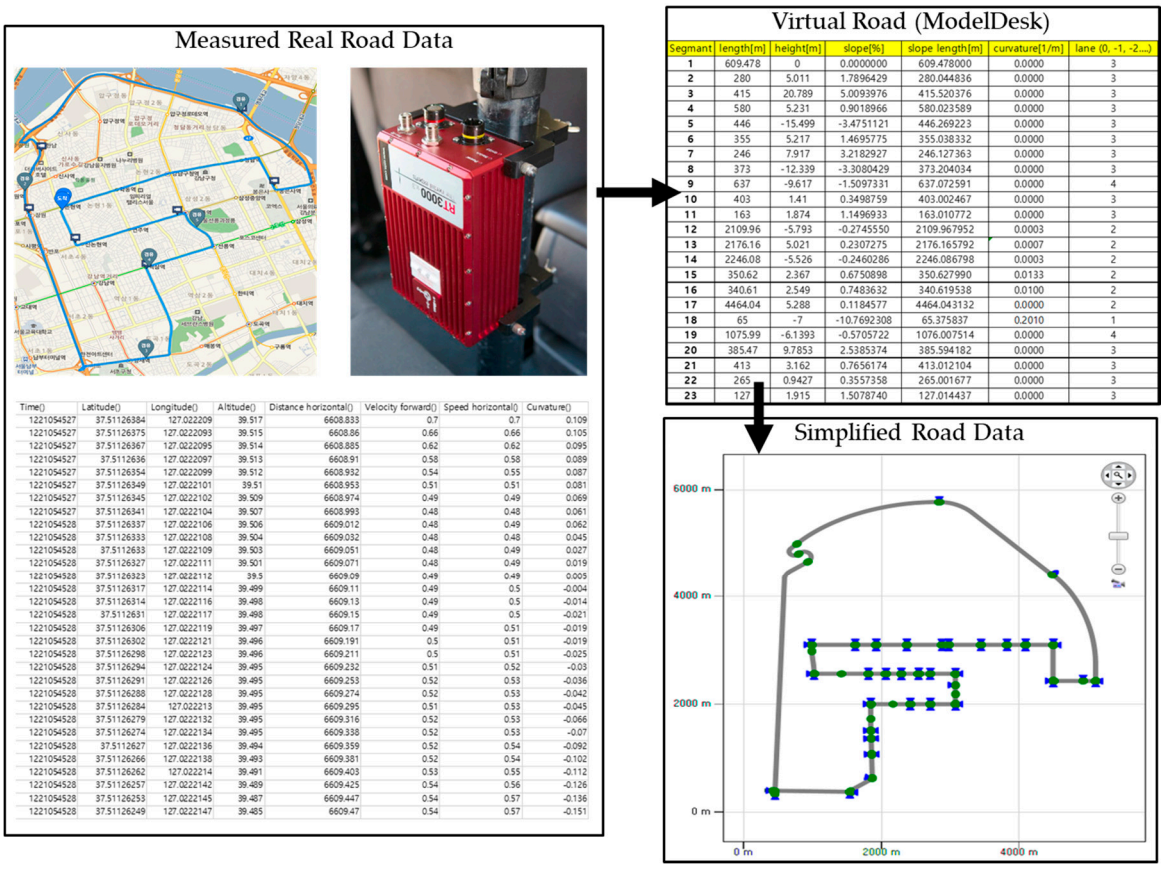

Time()	Latitude()	Longitude()	Altitude()	Distance horizontal()	Velocity forward()	Speed horizontal()	Curvature()
1221054527	37.51126384	127.022209	39.517	6608.833	0.7	0.7	0.109
1221054527	37.51126375	127.0222093	39.515	6608.86	0.66	0.66	0.105
1221054527	37.51126367	127.0222095	39.514	6608.885	0.62	0.62	0.095
1221054527	37.5112636	127.0222097	39.513	6608.91	0.58	0.58	0.089
1221054527	37.51126354	127.0222099	39.512	6608.932	0.54	0.55	0.087
1221054527	37.51126349	127.0222101	39.51	6608.953	0.51	0.51	0.081
1221054527	37.51126345	127.0222102	39.509	6608.974	0.49	0.49	0.069
1221054527	37.51126341	127.0222104	39.507	6608.993	0.48	0.48	0.061
1221054528	37.51126337	127.0222106	39.506	6609.012	0.48	0.49	0.062
1221054528	37.51126333	127.0222108	39.504	6609.032	0.48	0.48	0.045
1221054528	37.5112633	127.0222109	39.503	6609.051	0.48	0.49	0.027
1221054528	37.51126327	127.0222111	39.501	6609.071	0.48	0.49	0.019
1221054528	37.51126323	127.0222112	39.5	6609.09	0.49	0.49	0.009
1221054528	37.51126317	127.0222114	39.499	6609.11	0.49	0.5	-0.004
1221054528	37.51126314	127.0222116	39.498	6609.13	0.49	0.5	-0.014
1221054528	37.5112631	127.0222117	39.498	6609.15	0.49	0.5	-0.021
1221054528	37.51126306	127.0222119	39.497	6609.17	0.49	0.51	-0.019
1221054528	37.51126302	127.0222121	39.496	6609.191	0.5	0.51	-0.019
1221054528	37.51126298	127.0222123	39.496	6609.211	0.5	0.51	-0.025
1221054528	37.51126294	127.0222124	39.495	6609.232	0.51	0.52	-0.03
1221054528	37.51126291	127.0222126	39.495	6609.253	0.52	0.53	-0.036
1221054528	37.51126288	127.0222128	39.495	6609.274	0.52	0.53	-0.042
1221054528	37.51126284	127.022213	39.495	6609.295	0.51	0.53	-0.045
1221054528	37.51126279	127.0222132	39.495	6609.316	0.52	0.53	-0.066
1221054528	37.51126274	127.0222134	39.495	6609.338	0.52	0.53	-0.07
1221054528	37.5112627	127.0222136	39.494	6609.359	0.52	0.54	-0.092
1221054528	37.51126266	127.0222138	39.493	6609.381	0.52	0.54	-0.102
1221054528	37.51126262	127.022214	39.491	6609.403	0.53	0.55	-0.112
1221054528	37.51126257	127.0222142	39.489	6609.425	0.54	0.56	-0.126
1221054528	37.51126253	127.0222145	39.487	6609.447	0.54	0.57	-0.136
1221054528	37.51126249	127.0222147	39.485	6609.47	0.54	0.57	-0.151

Segment	length[m]	height[m]	slope[%]	slope length[m]	curvature[1/m]	lane (0, -1, -2,...)
1	609.478	0	0.0000000	609.478000	0.0000	3
2	280	5.011	1.7896429	280.044836	0.0000	3
3	415	20.789	5.0093976	415.520376	0.0000	3
4	580	5.231	0.9018966	580.023589	0.0000	3
5	446	-15.499	-3.4751121	446.269223	0.0000	3
6	355	5.217	1.4695775	355.038332	0.0000	3
7	246	7.917	3.2182927	246.127363	0.0000	3
8	373	-12.339	-3.3080429	373.204034	0.0000	3
9	637	-9.617	-1.5097331	637.072591	0.0000	4
10	403	1.41	0.3498759	403.002467	0.0000	3
11	163	1.874	1.1496933	163.010772	0.0000	3
12	2109.96	-5.793	-0.2745550	2109.967952	0.0003	2
13	2176.16	5.021	0.2307275	2176.165792	0.0007	2
14	2246.08	-5.526	-0.2460286	2246.086798	0.0003	2
15	350.62	2.367	0.6750898	350.627990	0.0133	2
16	340.61	2.549	0.7483632	340.619538	0.0100	2
17	4464.04	5.288	0.1184577	4464.043132	0.0000	2
18	65	-7	-10.7692308	65.375837	0.2010	1
19	1075.99	-6.1393	-0.5705722	1076.007514	0.0000	4
20	385.47	9.7853	2.5385374	385.594182	0.0000	3
21	413	3.162	0.7656174	413.012104	0.0000	3
22	265	0.9427	0.3557358	265.001677	0.0000	3
23	127	1.915	1.5078740	127.014437	0.0000	3

Figure 5. Process of virtual road implementation.

2.3. Simulation Scenario

Figure 6 shows the simulation scenario with the driving path, traffic light locations, and traffic jams. The driving path includes a motorway and an urban road, with speed limits of 80 km/h and 50 km/h, respectively. There are 11 traffic lights, and the traffic light cycle is the same as observed. The vehicle is operated by the driver by manipulating the driving controller, and the starting and ending points are fixed and follow the same path. The total driving distance is about 12.1 km. Also, the driver must obey the road speed limit and traffic signals.

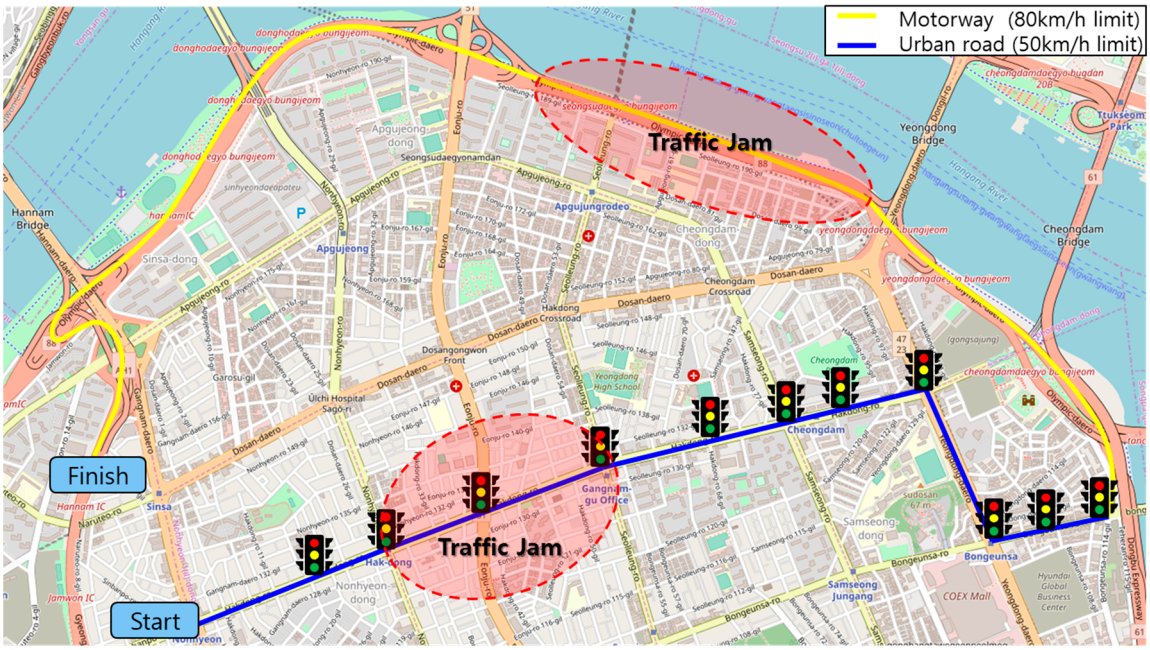

Figure 6. Simulation scenario with the driving path and traffic elements.

3. Energy Management Strategy

This section describes the proposed EMS. It consists of cooperative eco-driving (CED) guidance and an A-ECMS. It utilizes V2X information and road information for power distribution and guidance. The information acquired by V2X communication is traffic light state/remaining time and the average speed of the vehicle in front.

3.1. Cooperative Eco-Driving (CED) Guidance

In previous research [22], only traffic light speed assistance (TSA) using V2I communication has been applied. V2I communication information is provided in the form of SpaT (signal phase and timing) messages. It consists of the signal phase, the signal's remaining time, and the traffic light ID/location. TSA provides the possibility of passing a traffic light and the speed required to do so by considering the remaining time of the light and the distance from the light. Therefore, it was possible to reduce fuel consumption by reducing the stopping time in driving conditions with traffic lights or guiding the driver to know where to stop in advance. In this paper, curve speed assistance (CSA) and slope speed assistance (SSA) based on road information are added. In addition, speed information of vehicles ahead is acquired through V2V communication. Therefore, traffic jams can be recognized and prepared for in advance. CSA and traffic jam recognition can not only prevent accidents in real-world driving but can also be a way to improve fuel economy. Utilizing a variety of information, CED guidance not only provides eco-driving speeds, but also improves the timing of coasting driving to prevent unnecessary accelerator pedal use.

3.1.1. Curve Speed Assistance (CSA)

When a vehicle encounters a sharp curve, it needs to slow down to stay safe. CSA takes into account the curvature of the curve and calculates a safe speed limit, as shown in Figure 7. The goal is to provide this information to the driver to encourage safe driving on sharp curves. It also guides the driver when coasting before entering a curve to minimize brake use. This means that you can avoid sudden stops and reduce unnecessary use of the accelerator and brake pedals, which not only improves safety but also improves fuel economy. The curve speed limit is calculated as shown in Equation (1).

$$v_{lim,\mathrm{CSA}} = \max\left(\sqrt{\frac{\mu_{road}\, g}{\kappa}} - \Delta v_{safety}, v_{lim,min}\right) \tag{1}$$

$v_{\mathrm{lim,CSA}}$ is the curve speed limit for CSA. μ_{road} is the friction coefficient of the road and uses the default value from the dSPACE ASM. g is gravity acceleration. κ is road curvature. Δv_{safety} is the additional speed margin for safety (=5 km/h). $v_{lim,min}$ is the minimum speed limit (=12 km/h).

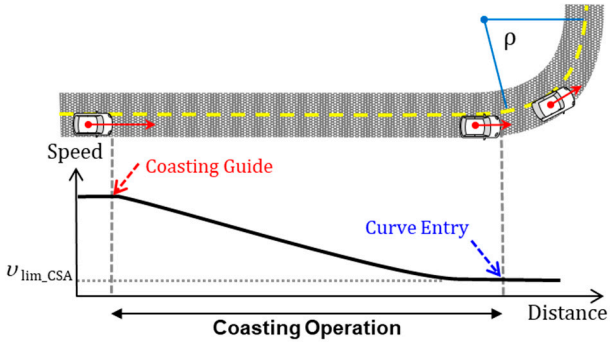

Figure 7. Scheme of curve speed assistance for eco-driving guidance.

3.1.2. Slope Speed Assistance (SSA)

SSA allows the driver to decelerate by coasting before the vehicle enters a downhill area, as shown in Figure 8. The vehicle is then accelerated by gravity on the slope to reach the slope exit speed. This reduces brake maneuvers on the slope. The slope entry speed is calculated by taking into account the average slope and length of the segment of road and the expected slope exit speed. It is assumed that there is no pedal intervention from the driver and that the engine clutch is disengaged. Since the entry speed is not known, the speed for calculating the drag force is assumed to be the exit speed after consideration for a margin of error. To calculate the slope entry speed, the driving resistance force F_R of the vehicle is calculated as shown in Equation (2) below.

$$\begin{aligned} F_R &= F_{roll} + F_{drag} + F_{grade} \\ &= -f_{roll}\, mg\cos\theta - 0.5 C_d\, A\rho {v_{exit}}^2 - mg\sin\theta \end{aligned} \tag{2}$$

where F_{roll} is the rolling resistance force, F_{drag} is the aerodynamics drag force, F_{grade} is the grade resistance force, f_{roll} is the rolling resistance coefficient, m is the vehicle mass, θ is the slope angle, C_d is the aerodynamics drag coefficient, A is the frontal area of the vehicle, and ρ is the air density.

The slope entry speed $v_{ent,\mathrm{SSA}}$ is calculated using the trapezoidal rule for approximation of integrals. It uses the average slope of the segment of road and assumes an ideal situation where only F_R exists. Using the driving resistance force F_R, the exit speed v_{exit}, and the slope length d_{seg}, the slope entry speed is calculated as follows.

$$v_{ent,\mathrm{SSA}} = \sqrt{{v_{exit}}^2 - 2 d_{seg} \frac{F_R}{m}} \tag{3}$$

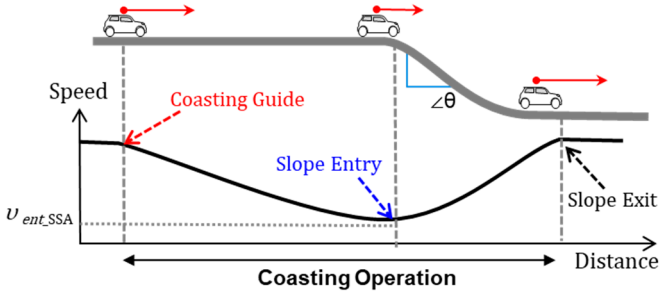

Figure 8. Scheme of slope speed assistance for eco-driving guidance.

3.1.3. Coasting Assistance (CA)

As shown in Figure 9, the purpose of CA is to provide the driver with the timing of coasting initiation. It works in situations where deceleration is required by TSA, CSA, SSA, or the speed of the vehicle ahead. When it reaches a location where coasting is required, it calculates the coasting distance to guide the driver. The coasting distance d_C can be calculated using the trapezoidal rule for approximation of integrals, as shown in Equation (4) below.

$$d_C = \frac{m}{2F_R}\left({v_{C,end}}^2 - {v_{C,start}}^2\right) \tag{4}$$

where v_{C_start} is the expected speed of the vehicle at the start of coasting and v_{C_end} is the speed to be reached after coasting, which uses the minimum of the following: curve speed limit, slope entry speed, the average speed of the vehicle in front of you, the guide speed according to TSA, and the speed limit of the road.

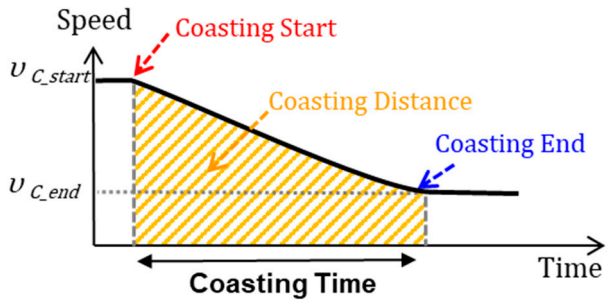

Figure 9. Scheme of coasting assistance for eco-driving guidance.

3.1.4. Cooperative Eco-Driving Speed and Guide Signals

The guide speed provided to the driver is determined by considering the assistance speeds (calculated by CSA, SSA, and TSA), the road speed limit, and the average speed of the vehicles ahead. The CED speed v_{CED} is determined as follows.

$$v_{\mathrm{CED}} = \min\left(v_{lim,\mathrm{CSA}}, v_{ent,\mathrm{SSA}}, v_{\mathrm{TSA}}, v_{lim,road}, v_{avg,v2v}\right) \tag{5}$$

The guide signal consists of three lights: green, yellow, and red. These are described in detail below:

- Green light: This is a situation where there are no curves, slopes, or traffic jams. The driver maneuvers the pedals so that the vehicle speed follows the guide speed. It also includes situations where TSA determines that the vehicle will be able to pass through the intersection. In this case, the speed to pass through the intersection is provided.
- Yellow light: When there is a curve, slope, or traffic jam ahead, it guides the driver to coast. In this case, the driver can coast until the guide speed is reached without pedal control.

- Red light: This is a situation where TSA has determined that you will be stopped by an upcoming traffic light. This requires the driver to coast and then stop at the intersection.

Figure 10 shows dSPACE MotionDesk visualizing the simulation environment. Here, we configure the UI for visual guidance to display the guide speed and guide signal.

Figure 10. Visual guidance for cooperative eco-driving in the MotionDesk simulation.

To summarize, CED guidance works as shown in Figure 11. It utilizes road segment information, vehicle data, and V2X data as information. With this information, it provides guide speeds and guide signals to the driver for eco-driving.

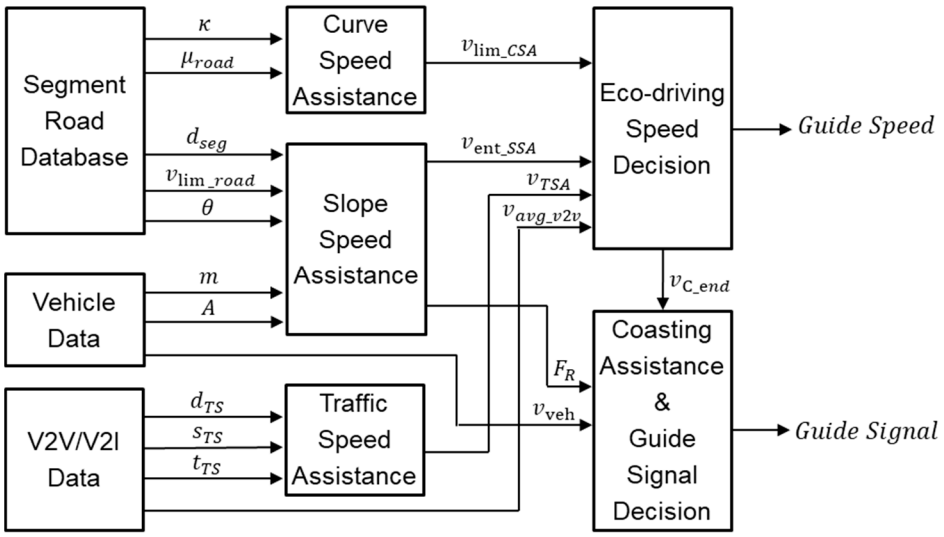

Figure 11. Structure of the cooperative eco-driving guidance workflow.

3.2. Adaptive Equivalent Consumption Minimization Strategy with Target SOC

3.2.1. Target SOC Decision with Road Information

The main purpose of determining the target SOC is to ensure that the battery does not overcharge or overdischarge by using the road information ahead. For example, a downhill road ahead may cause the battery to overcharge and not be able to charge all of the regenerative braking energy. In this case, you can drain the battery in advance to make sure it is fully charged. You may also encounter a situation where the vehicle is driving in HEV mode due to a low SOC on a road that can be driven in EV mode.

The estimated driving speed to calculate the SOC change on a road segment considers the speed limit and curvature of the road. It is assumed that vehicles travel at a constant speed on a road segment, with speed limited by the road. Therefore, the estimated average speed is as follows.

$$v_{avg,seg} = \min(v_{lim,\mathrm{CSA}},\ v_{lim,road}) \tag{6}$$

Substitute Equation (6) into Equation (2) to calculate the driving resistance $F_{R,est}$.

$$\begin{aligned} F_{R,est} &= F_{roll} + F_{drag} + F_{grade} \\ &= -f_{roll}\ mg\cos\theta - 0.5C_d\ A\rho {v_{avg,seg}}^2 - mg\sin\theta \end{aligned} \tag{7}$$

Assuming the vehicle is traveling at a constant speed, the tractive force $F_{tr,est}$ can be expressed as

$$F_{tr,est} = -F_{R,est} \tag{8}$$

From the tractive force, we then calculate the estimated torque and angular velocity of MG1 and determine the estimated driving mode of the vehicle accordingly.

$$T_{MG1,est} = R_{whl} F_{tr,est} r_{whl2MG1} \tag{9}$$

$$\omega_{MG1,est} = \frac{v_{avg,est}}{R_{whl} r_{whl2MG1}} \tag{10}$$

$$b_{mode,est} = \begin{cases} 1\ , & T_{MG1,est} > T_{EV,lim}(\omega_{MG1,est}) \\ 2\ , & T_{EV,lim}(\omega_{MG1,est}) \geq T_{MG1,est} > 0 \\ 3\ , & 0 \geq T_{MG1,est} \end{cases} \tag{11}$$

where $T_{MG1,est}$ is the estimated torque of MG1, $\omega_{MG1,est}$ is the estimated angular velocity of MG1, R_{whl} is the wheel radius, $r_{whl2MG1}$ is the gear ratio from the wheel to MG1, and $T_{EV,lim}(\omega_{MG1,est})$ is the EV mode torque limit according to the estimated MG1 angular velocity. If the estimated driving mode $b_{mode,est}$ is 1, it is HEV mode; if it is 2, it is EV mode; and if it is 3, it is regenerative braking mode.

Next, we calculated the estimated SOC change of the battery, $\Delta SOC_{bat,est}$. When the driving mode is EV or regen mode, only MG1 is used to drive or brake, and when it is HEV mode, the engine is assumed to be running at OOL torque, and the extra torque is driven by MG1. The angular velocity of the engine is the same as MG1. To summarize, the estimated usage of the battery is calculated from the tractive force. $\Delta SOC_{bat,est}$ is calculated as follows.

$$P_{bat,est} = \begin{cases} T_{MG1,est}\omega_{MG1,est}\eta_{e,avg}, & b_{mode,est} > 1 \\ (T_{MG1,est} - T_{OOL}(\omega_{MG1,est}))\omega_{MG1,est}\eta_{e,avg}, & b_{mode,est} = 1 \end{cases} \tag{12}$$

$$\Delta SOC_{bat,est} = -\frac{P_{bat,est}\ d_{seg}}{3600 V_{bat} Q_{bat} v_{avg,est}}. \tag{13}$$

where $P_{bat,est}$ is the estimated battery power, $\eta_{e,avg}$ is the average efficiency of energy transfer between MG1 and the battery, $T_{OOL}(\omega_{MG1,est})$ is the engine OOL torque, V_{bat} is the battery voltage, and Q_{bat} is the battery capacity. The engine speed is equal to the angular velocity of MG1. Equations (6)–(13) are calculated for the three road segments ahead, which we define as segment 1, segment 2, and segment 3, respectively. $\Delta SOC_{bat,est}$ for each is expressed as ΔSOC_1, ΔSOC_2, and ΔSOC_3.

The target SOC is determined by reflecting SOC_0, the battery charge status when entering the next road segment. Figure 12 shows the main idea of the target SOC decision. As shown in Figure 12a, the main purpose is to determine the target SOC at the end of segment 1, which is the next road segment. In normal situations, SOC_0 and ΔSOC_1 are added together when entering segment 1. The SOC range of the battery must be bounded by upper/lower limits considering its lifetime, efficiency, voltage, etc. This leads to the

need to adjust the target SOC according to the conditions of the road to be traveled. In the situation in Figure 12b, when driving in EV mode in segment 2, it is expected that the SOC lower limit will be exceeded due to insufficient battery capacity. In response, the target SOC is adjusted in segment 1, which is HEV mode, to enable full EV driving in segment 2. In the case of Figure 12c, regenerative braking is expected to be limited to prevent overcharging when driving in regen mode in segment 3. In response, the target SOC of segment 1 is adjusted to be lower. Therefore, all the regenerative braking energy can be obtained in segment 3. This adjustment can prevent situations where EV mode and regenerative braking are limited. The target SOC decision algorithm is shown in Figure 13.

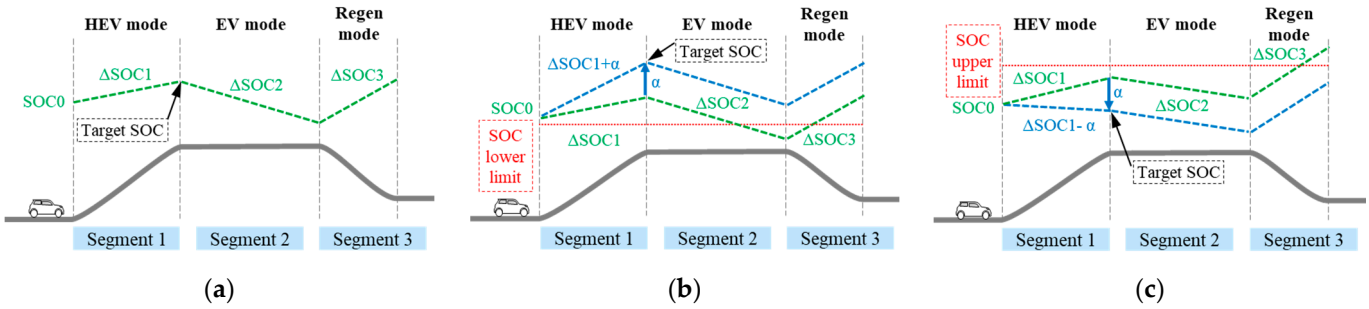

Figure 12. Main ideas of target SOC decisions: (**a**) inside of the boundary; (**b**) outside of the lower limit; (**c**) outside of the upper limit.

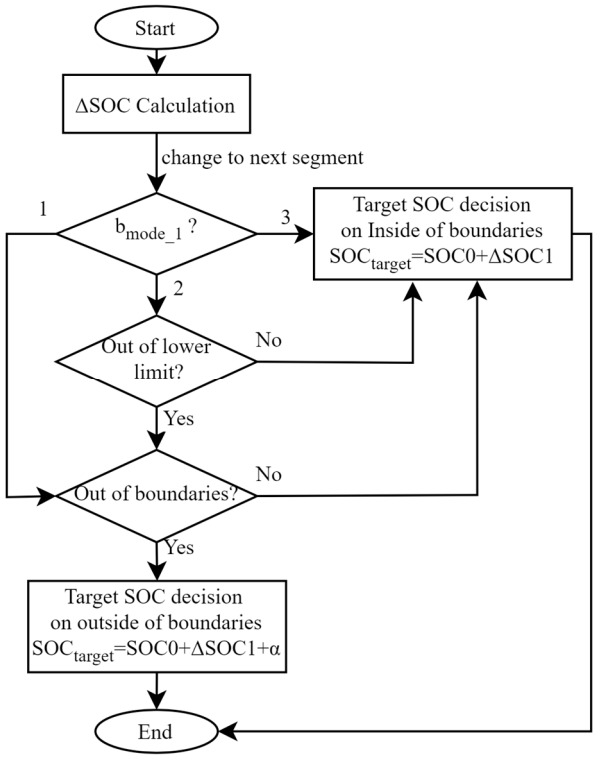

Figure 13. Flowchart of the target SOC decision algorithm.

3.2.2. Adaptive ECMS

In this paper, we use an A-ECMS, which is one of the various optimal power distribution control methods. The target SOC derived from the road segment information is reflected in the equivalence factor (EF). This allows for the charge–discharge tendency to

be adjusted according to the information of the road segment. The equivalent factor s of a conventional ECMS and an A-ECMS is as follows.

$$s = \begin{cases} s_0 & , \ ECMS \\ s_0 + K_p\left(SOC_{target} - SOC_0\right) + K_i\left(SOC_{target} - SOC_0\right) & , \ Adaptive\ ECMS \end{cases} \quad (14)$$

where s_0 is the initial EF and K_p and K_i are the coefficients of the PI controller.

Next, a quasistationary model of the vehicle was used to calculate the energy consumption required from fuel and the battery in relation to the driver's required torque [23]. In this paper, the control input candidates (u_{grid}) used 61 grids. As a result, the power candidates $P_{f,grid}$ for fuel and $P_{b,grid}$ for the battery are calculated, and the cost function J is defined as follows.

$$J = P_{f,grid} + sP_{b,grid} \quad (15)$$

The control input for which the cost function J has a minimum value is

$$u^* = \arg\min_{u_{grid}} J \quad (16)$$

where u^* is the optimal power distribution ratio. Therefore, the engine torque command $T_{eng,cmd}$ and motor torque command $T_{MG,cmd}$ are calculated from the required torque T_{req} as follows.

$$T_{eng,cmd} = u^* T_{req} \quad (17)$$

$$T_{MG,cmd} = \left(1 - u^*\right) T_{req} \quad (18)$$

$T_{eng,cmd}$ and $T_{MG,cmd}$ are sent to the controllers of the engine and motor, respectively. The workflow of the A-ECMS with target SOC is shown in Figure 14.

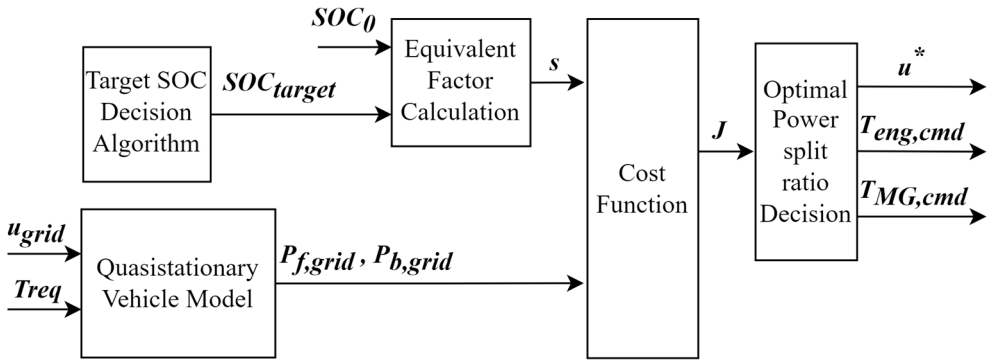

Figure 14. Workflow of the A-ECMS with target SOC.

4. Test Results Using the IDHIL Simulator

For the evaluation of the CED guidance and A-ECMS mentioned in Section 3, simulations were performed on a test bench consisting of the IDHIL simulator environment from Section 2. Only one driver participated to minimize driver variables. The driving path and traffic conditions were the same as in the scenario in Section 2.3. For comparison, the case with no CED guidance and the ECMS with a fixed EF value (normal PHEV) is also included. The simulation was performed four times each for both the connected PHEV and normal PHEV cases. The simulation results are shown below in Figure 15 for vehicle speed, Figure 16 for SOC, and Figure 17 for fuel consumption.

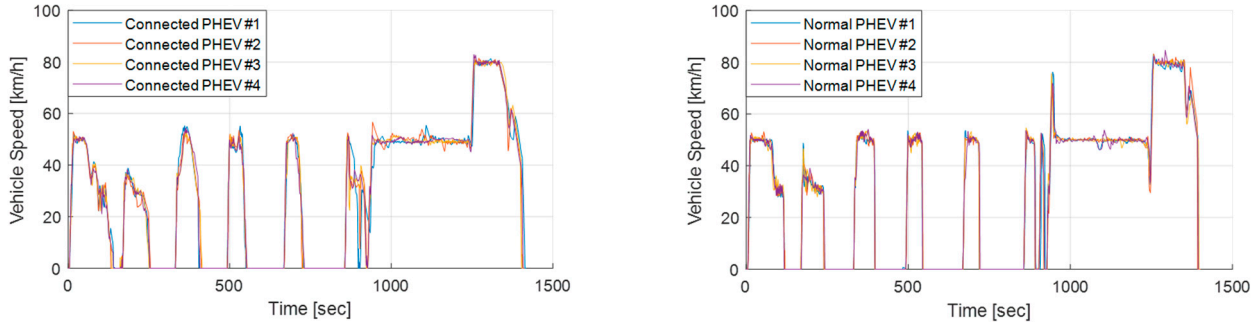

(**a**) (**b**)

Figure 15. Vehicle speed results: (**a**) connected PHEV; (**b**) normal PHEV.

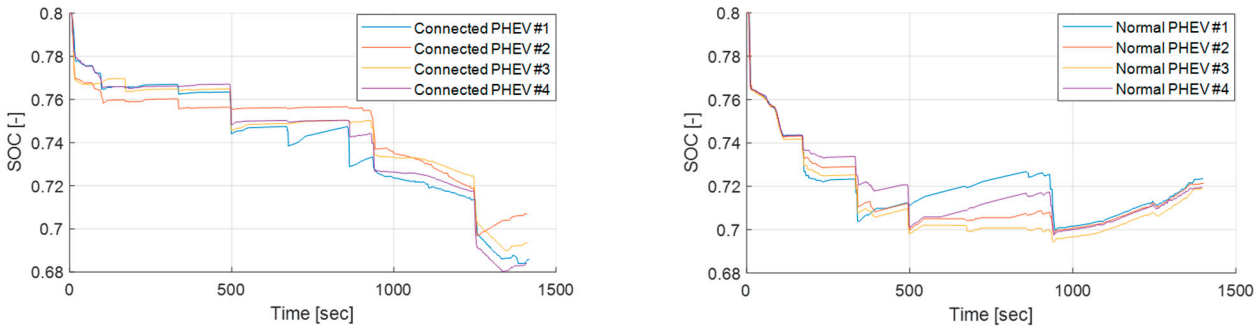

(**a**) (**b**)

Figure 16. SOC results: (**a**) connected PHEV; (**b**) normal PHEV.

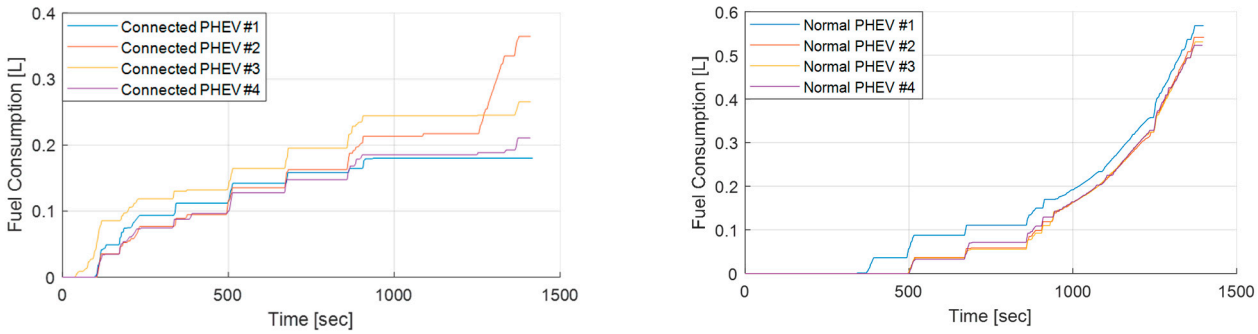

(**a**) (**b**)

Figure 17. Total fuel consumption results: (**a**) connected PHEV; (**b**) normal PHEV.

Table 2 shows the results of the simulation and the fuel consumption calculated from it. Here, we can see the total driving range, the final SOC of the battery at the end of the simulation, and the fuel consumption. To calculate the PHEV's fuel economy, we calculate the equivalent fuel consumption $V_{fuel,e}$ based on the battery usage as follows.

$$V_{fuel,e} = \frac{\left(SOC_{init} - SOC_{final}\right) V_{bat} Q_{bat}}{\alpha} \tag{19}$$

where α (=8.9 kWh/L) is the conversion factor for converting 1 L of gasoline to electrical energy [24]. SOC_{init} and SOC_{final} are the initial and final SOCs. The numerator is the electrical energy consumption as the SOC changes. The total fuel consumption was calculated by adding the fuel consumption of the engine and $V_{fuel,e}$. The average fuel consumption of the connected PHEV was 29.31 km/L, while the average fuel consumption of the normal

PHEV was 18.28 km/L. The difference in fuel economy is 11.03 km/L, and the difference in the improvement rate is 60.28%.

Table 2. Simulation results: fuel economy.

Case	Total Distance	Final SOC	Fuel Consumption	Equivalent Fuel Consumption	Total Fuel Consumption	Fuel Economy
Connected PHEV #1	12.099 [km]	0.6856 [-]	0.1801 [L]	0.1754 [L]	0.3555 [L]	34.03 [km/L]
Connected PHEV #2	12.091 [km]	0.7069 [-]	0.3646 [L]	0.1427 [L]	0.5073 [L]	23.83 [km/L]
Connected PHEV #3	12.1 [km]	0.6935 [-]	0.2655 [L]	0.1633 [L]	0.4288 [L]	28.22 [km/L]
Connected PHEV #4	12.101 [km]	0.684 [-]	0.2108 [L]	0.1778 [L]	0.3886 [L]	31.14 [km/L]
Normal PHEV #1	12.102 [km]	0.7235 [-]	0.5681 [L]	0.1173 [L]	0.6854 [L]	17.66 [km/L]
Normal PHEV #2	12.104 [km]	0.7212 [-]	0.5413 [L]	0.1208 [L]	0.6621 [L]	18.28 [km/L]
Normal PHEV #3	12.1 [km]	0.719 [-]	0.531 [L]	0.1242 [L]	0.6552 [L]	18.47 [km/L]
Normal PHEV #4	12.106 [km]	0.7196 [-]	0.5229 [L]	0.1233 [L]	0.6462 [L]	18.73 [km/L]

These results show the difference between a connected PHEV and a normal PHEV. It shows the difference in driving speed depending on whether CED guidance is used or not. We can also see the difference in fuel and battery usage tendencies with and without the A-ECMS. This is mentioned in more detail in Sections 4.1 and 4.2

4.1. Comparison of Engine Operating Points between Connected and Normal PHEVs

To analyze the fuel economy improvement effect of the A-ECMS, we compared the engine operating points of connected and normal PHEVs. Figure 18 shows the engine operating points of a connected PHEV. Figure 19 shows the engine operating points of a normal PHEV. In both cases, we can see that the engine operates within a similar range. The difference is that the engine runs more frequently in the normal PHEV.

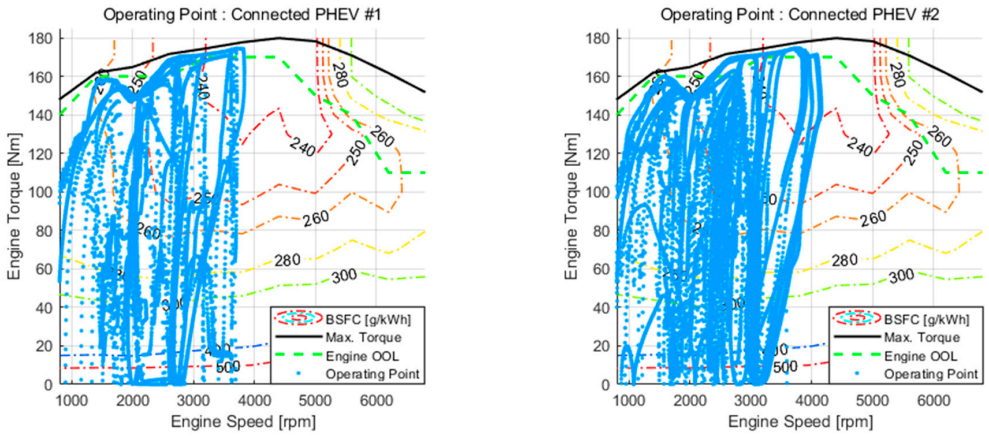

(**a**) (**b**)

Figure 18. *Cont.*

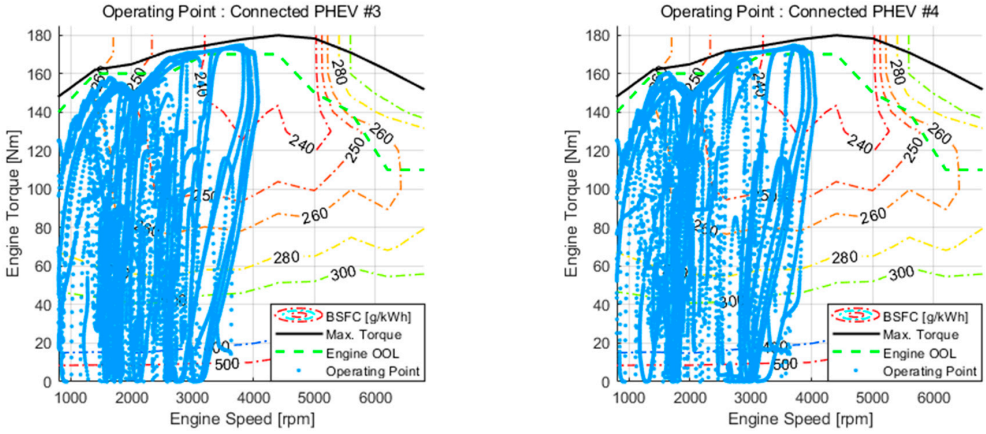

(**c**) (**d**)

Figure 18. Engine operating points of a connected PHEV: (**a**) #1; (**b**) #2; (**c**) #3; (**d**) #4.

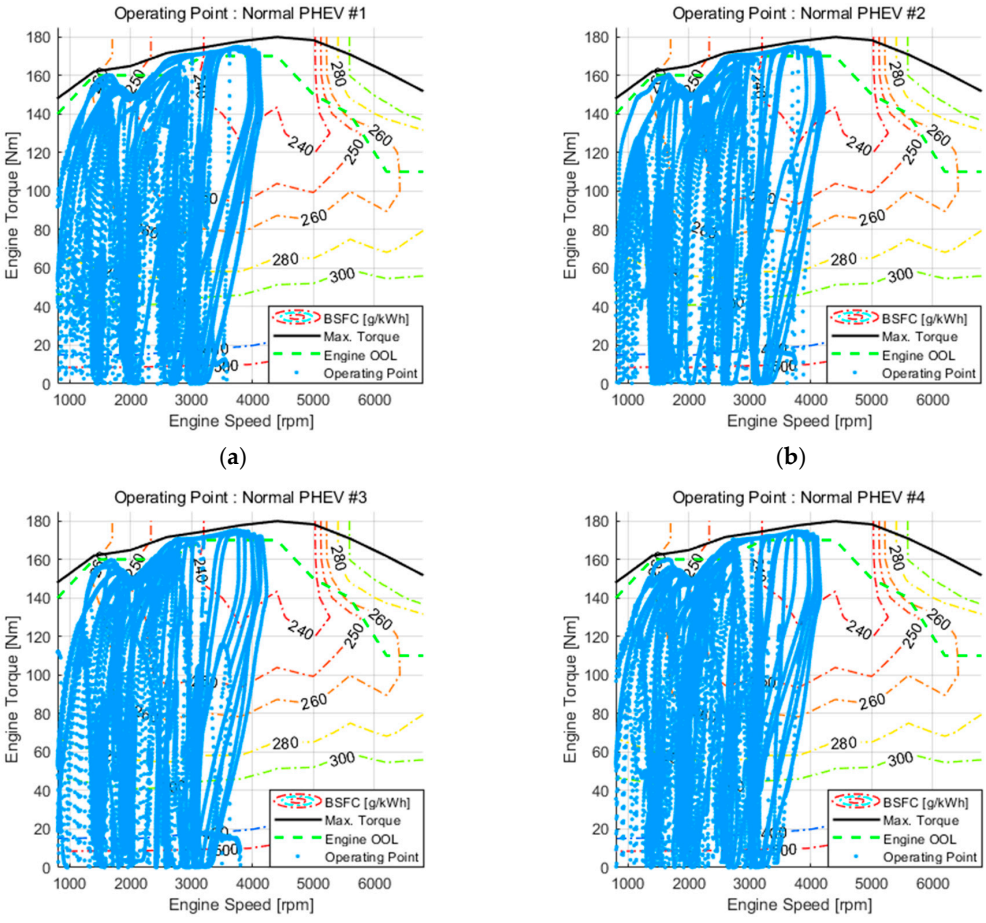

(**a**) (**b**)

(**c**) (**d**)

Figure 19. Engine operating points of a normal PHEV: (**a**) #1; (**b**) #2; (**c**) #3; (**d**) #4.

To analyze engine behavior in more detail, we plotted the frequency of engine operation as a function of BSFC in Figures 20 and 21. In the case of the connected PHEV, the engine mainly operated at a low level of BSFC (around 240–300), while in the case of the normal PHEV, the percentage of engine operation was relatively high in terms of BSFC (around 350). In other words, it can be seen that the connected PHEV operated in the low BSFC region.

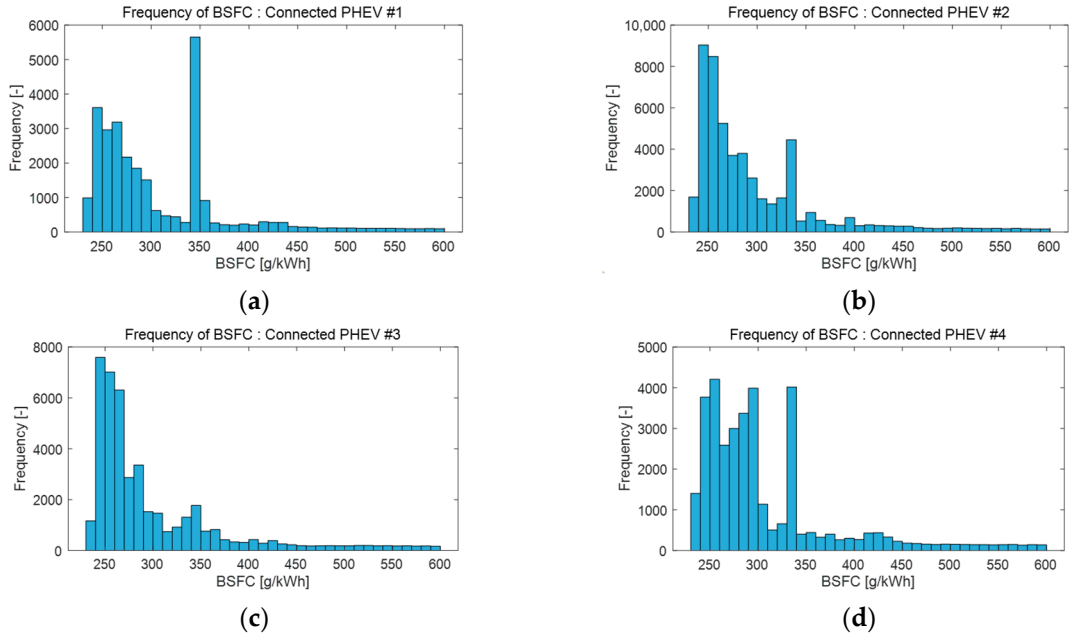

Figure 20. Frequency of BSFC for the connected PHEV: (**a**) #1; (**b**) #2; (**c**) #3; (**d**) #4.

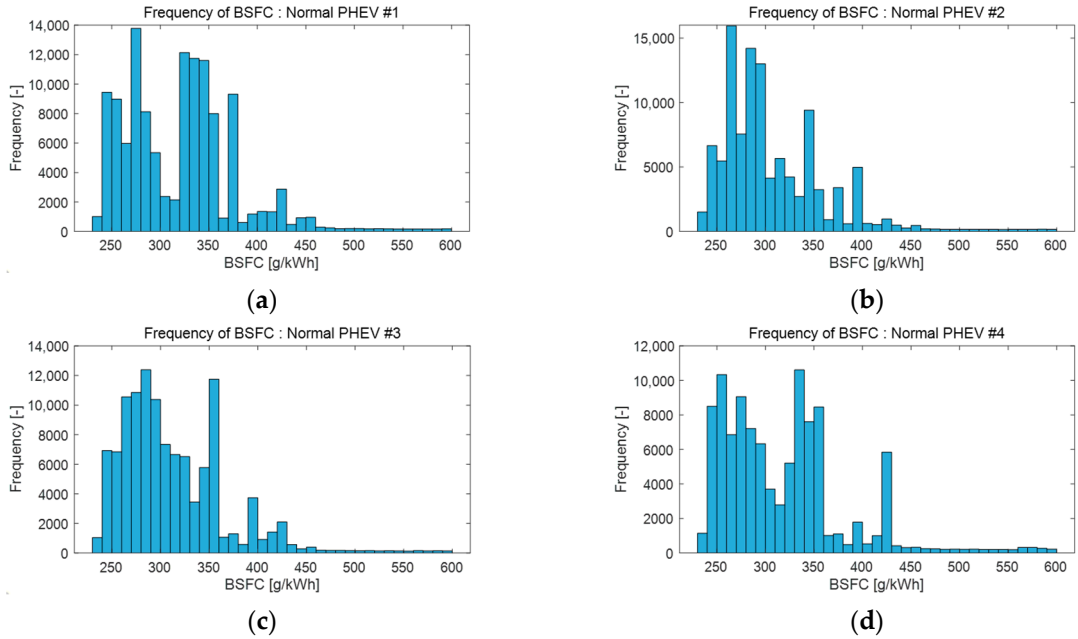

Figure 21. Frequency of BSFC for the normal PHEV: (**a**) #1; (**b**) #2; (**c**) #3; (**d**) #4.

To see this clearly, we derived the overall frequency of connected and normal PHEVs, as shown in Figure 22. We categorized them into four levels based on BSFC: very low (BSFC: 230–245), low (BSFC: 245–260), medium (BSFC: 260–300), and high (BSFC: 300–600). The very low level, which is the most energy efficient, has a difference of 5.43%. At the low level, the difference is 10.7%. Based on these results, we can see that the engine operated at higher efficiency in the connected PHEV with the A-ECMS than in the normal PHEV.

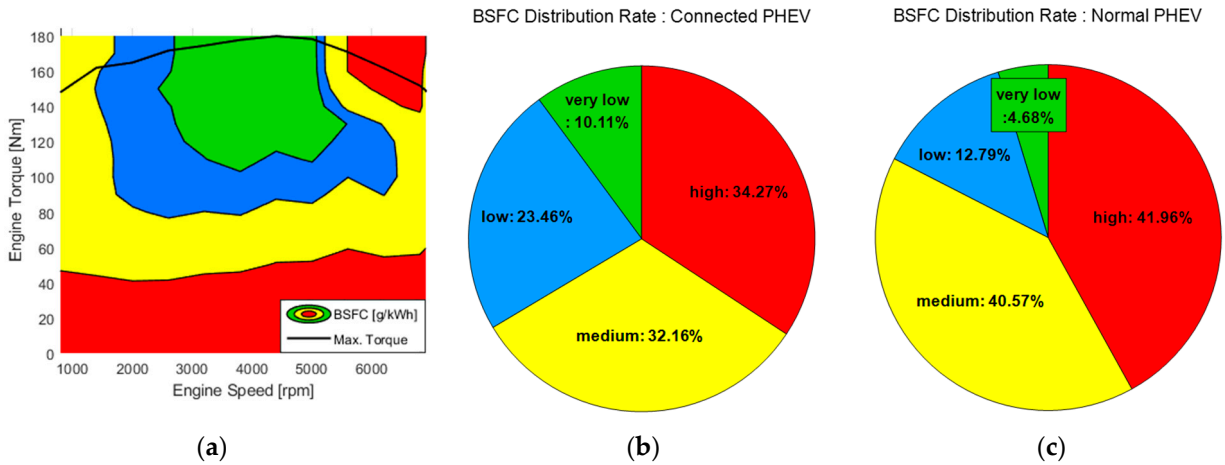

(**a**) (**b**) (**c**)

Figure 22. Comparison of BSFC distribution rates: (**a**) four-level classification of BSFC; (**b**) connected PHEV; (**c**) normal PHEV.

4.2. Differences due to Target SOC in the A-ECMS

Figure 23 shows the SOC of normal PHEV #3 and connected PHEV #2. They appear to be very different, but a closer look reveals that their charge/discharge tendencies are similar: they each discharge in the same interval, but sometimes the electrical energy usage is limited by the target SOC, as in Figure 23b. In other words, the charge/discharge tendency is the same but the amount of charge/discharge is different. On the other hand, there are cases where the charge/discharge tendencies are opposite, as shown in Figure 23c where the connected PHEV has a discharge tendency and the normal PHEV has a charge tendency. The target SOC in this study is determined for each road segment, rather than a profile as was the case in [25]. This has the advantage of simplicity and low computational load. However, the fuel economy performance is lower compared to the SOC profile. In addition, the long initialization period of SOC_0 causes the error between actual SOC and target SOC to be larger. Nevertheless, it can be seen that the charge/discharge tendency changes significantly when compared to a normal PHEV. The connected PHEV using the A-ECMS with a target SOC adjusts the charge/discharge amount and the tendency of the battery according to the information of the road to be traveled in the future. Therefore, it can perform more efficient power distribution than a normal PHEV that only considers the torque demanded by the driver's pedal operation and the vehicle state.

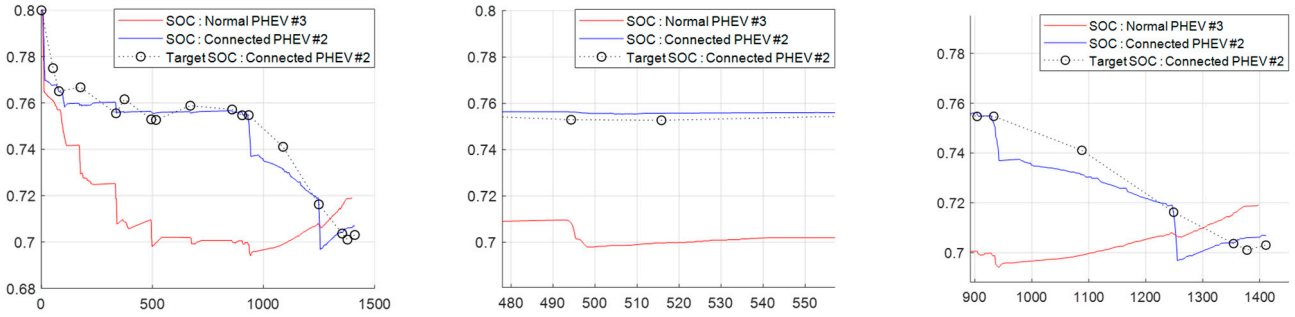

(**a**) (**b**) (**c**)

Figure 23. Comparison of SOC between normal PHEV #3 and connected PHEV #2 with target SOC: (**a**) entire time; (**b**) 480–560 s; (**c**) 900–1450 s.

4.3. Differences due to Cooperative Eco-Driving Guidance

We next compared the driving speed of the vehicles with and without CED guidance. In Figure 24a, the driving speeds of the connected PHEV and normal PHEV differ at certain

points. In Figure 24b, the normal PHEV makes a sharp stop as the light turns red, while the connected PHEV decelerates slowly by coasting. In Figure 24c, the connected PHEV realizes that the light ahead is about to turn green and decelerates to pass through the intersection without stopping, while the normal PHEV accelerates again after stopping at the intersection. In Figure 24d, the normal PHEV tries to accelerate to the speed limit of 80 km/h and is then slowed down by the traffic jam. However, the connected PHEV only accelerates to 50 km/h, the average speed of the traffic jam. In Figure 24e, a traffic jam is encountered on an urban road. The connected PHEV slowed down by coasting from about 57 s to 71 s. The normal PHEV slowed down by using some braking. In Figure 24f, the connected PHEV encounters a sharp curve later in the trip. The connected PHEV decelerates by coasting from approximately 1334 s to 1353 s, while the normal PHEV decelerates sharply by braking before entering the curve.

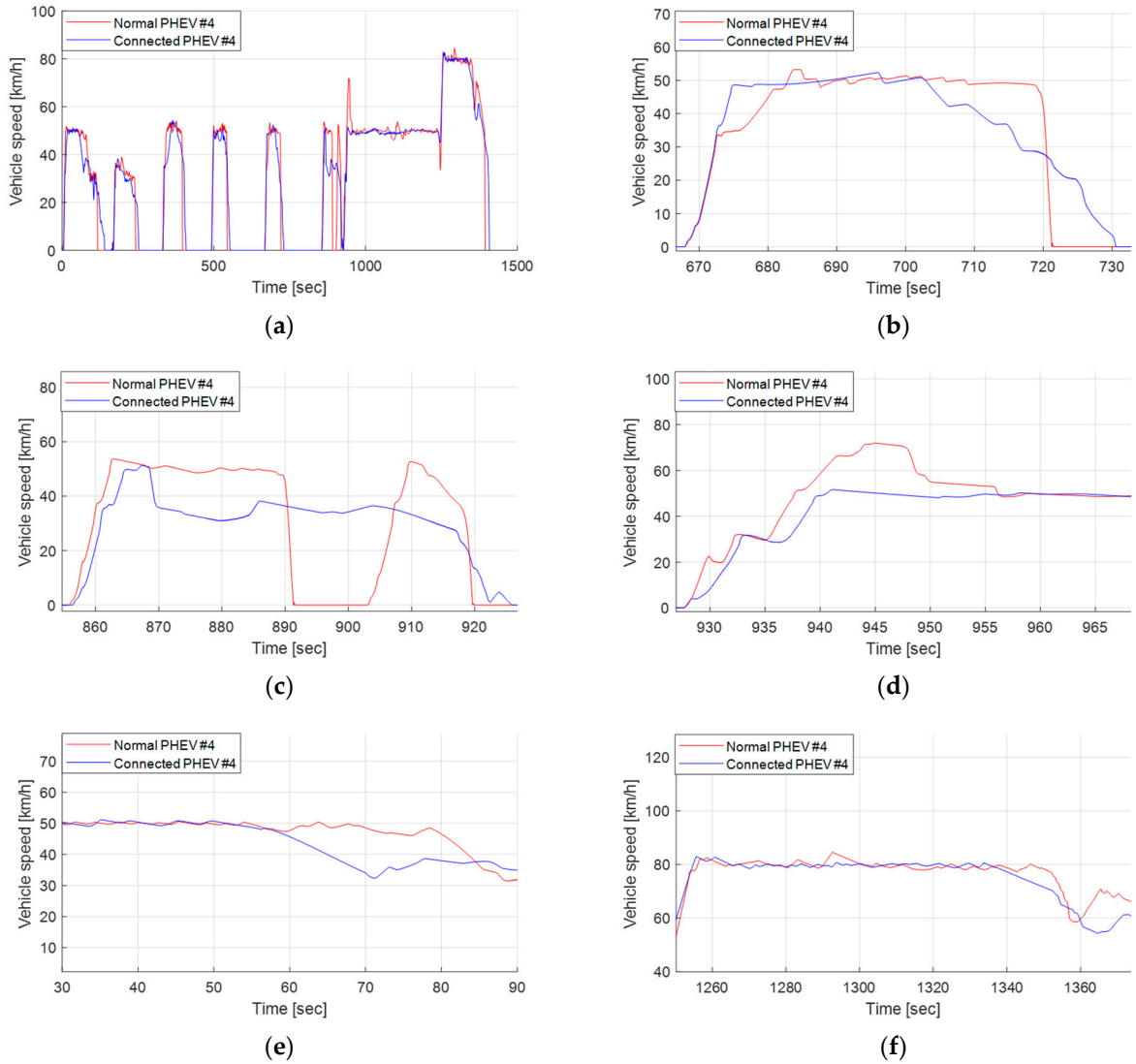

Figure 24. Comparison of driving speed between normal PHEV #4 and connected PHEV #4: (**a**) entire time; (**b**) 665–735 s; (**c**) 850–925 s; (**d**) 925–970 s; (**e**) 30–90 s; (**f**) 1270–1375 s.

The main purpose of CED guidance Is to reduce unnecessary deceleration. Looking at Table 3, you can see that the regenerative braking energy of a normal PHEV is higher, which means that the brake pedal has been pressed more and that energy has to be expended to accelerate again. If it were an internal combustion engine vehicle without regenerative braking, all of this energy would have been lost.

Table 3. Simulation results: regenerative braking energy.

Case	Connected PHEV	Normal PHEV
#1	24,183.69 [J]	145,252.51 [J]
#2	52,978.61 [J]	144,172.89 [J]
#3	48,528.40 [J]	130,616.57 [J]
#4	34,439.04 [J]	141,808.66 [J]

5. Discussion

In this paper, an EMS combining CED guidance and an A-ECMS was evaluated using the IDHIL simulator, which integrates a VANET simulator, V2X communication devices, and a vehicle simulation environment. CED guidance provides guide speeds and guide signals to the driver by considering road information (curvature, slope, distance, limit speed) and V2X communication information (traffic light, surrounding vehicle information). The A-ECMS performs optimal power distribution control by applying the target SOC derived based on road information to the equivalence factor. The connected PHEV with the proposed EMS was compared to a normal PHEV without eco-driving and with a conventional ECMS. The connected PHEV showed a fuel economy improvement of 60.28% compared to the normal PHEV. This equates to an average reduction in CO_2 emissions of 0.54 kg (36.57%). We came to the following conclusions from our simulation results.

- By driving with CED guidance using V2X communication and road information, brake and acceleration pedal usage is reduced, which can be seen through regenerative braking energies and engine operating points. This in turn reduces energy loss and the usage of vehicle systems.
- We can see the change in engine behavior by applying an A-ECMS using road information. Based on the road information, the target SOC was determined and reflected in the equivalent factor. As a result, the engine operated more often in areas with lower BSFC (higher efficiency).
- CED guidance encourages drivers to drive more efficiently, and the A-ECMS enables engines to operate more efficiently. We have found that the integration of CED guidance and the A-ECMS can be synergistic in terms of improving fuel efficiency.

Although we confirmed the improvement in fuel economy from the test results, further studies are needed to further improve fuel economy by utilizing the IDHIL simulator test bench with a connected vehicle environment. The first is to apply detailed road information in real time. In order to apply road information when driving in a real environment, real-time information must be guaranteed. In addition, applying a trajectory-based SOC reference using detailed road information will show a higher fuel efficiency improvement effect [26]. The second is to evaluate various EMS methods. EMSs for connected (P)HEVs have been well researched, but validation in a real V2X communication environment is lacking. Therefore, the IDHIL simulator can be used to test existing methods to validate the applicability and performance of existing EMSs in real-world V2X environments. Finally, application of an autonomous driving system should be verified. One of the problems that reduces the performance of eco-driving is human driver error. Since driver behavior is unpredictable and inconsistent, the performance of eco-driving systems cannot be guaranteed. Therefore, if an autonomous driving system is applied, its performance can be guaranteed because its ability to follow the reference speed is increased.

Author Contributions: Formal analysis, S.H.; project administration, S.H. and H.L.; software, S.H.; validation, S.H.; investigation, S.H.; writing—original draft preparation, S.H.; writing—review and editing, S.H. and H.L.; supervision, H.L. All authors have read and agreed to the published version of the manuscript.

Funding: This research received no external funding.

Data Availability Statement: Not applicable.

Acknowledgments: This work was supported by the Industrial Strategic Technology Development Program (20010132, Development of the Systematization Technology of an E-Powertrain Core Parts Development Platform for Expanding the Industry of xEV Parts) funded By the Ministry of Trade, Industry & Energy (MOTIE, Korea).

Conflicts of Interest: The authors declare no conflict of interest.

References

1. Zhang, P.; Zhang, H.; Sun, X.; Li, P.; Zhao, M.; Xu, S.; Jiao, X.; Sun, Z.; Zhang, T. Research on Carbon Emission Standards of Automobile Industry in BRI Participating Countries. *Clean. Responsible Consum.* **2023**, *8*, 100106. [CrossRef]
2. Banvait, H.; Anwar, S.; Chen, Y. A Rule-Based Energy Management Strategy for Plug-in Hybrid Electric Vehicle (PHEV). In Proceedings of the 2009 American Control Conference, St. Louis, MI, USA, 10–12 June 2009; IEEE: St. Louis, MO, USA, 2009; pp. 3938–3943.
3. Rajagopalan, A.; Washington, G. *Intelligent Control of Hybrid Electric Vehicles Using GPS Information*; SAE Technical Paper Series; SAE International: Warrendale, PA, USA, 2002.
4. Lin, C.-C.; Peng, H.; Grizzle, J.W.; Kang, J.-M. Power Management Strategy for a Parallel Hybrid Electric Truck. *IEEE Trans. Control Syst. Technol.* **2003**, *11*, 839–849. [CrossRef]
5. Delprat, S.; Lauber, J.; Guerra, T.M.; Rimaux, J. Control of a Parallel Hybrid Powertrain: Optimal Control. *IEEE Trans. Veh. Technol.* **2004**, *53*, 872–881. [CrossRef]
6. Barsali, S.; Miulli, C.; Possenti, A. A Control Strategy to Minimize Fuel Consumption of Series Hybrid Electric Vehicles. *IEEE Trans. Energy Convers.* **2004**, *19*, 187–195. [CrossRef]
7. Kessels, J.T.B.A.; Koot, M.W.T.; van den Bosch, P.P.J.; Kok, D.B. Online Energy Management for Hybrid Electric Vehicles. *IEEE Trans. Veh. Technol.* **2008**, *57*, 3428–3440. [CrossRef]
8. Enang, W.; Bannister, C. Modelling and Control of Hybrid Electric Vehicles (A Comprehensive Review). *Renew. Sustain. Energy Rev.* **2017**, *74*, 1210–1239. [CrossRef]
9. Yan, F.; Wang, J.; Du, C.; Hua, M. Multi-Objective Energy Management Strategy for Hybrid Electric Vehicles Based on TD3 with Non-Parametric Reward Function. *Energies* **2022**, *16*, 74. [CrossRef]
10. Zhang, F.; Hu, X.; Langari, R.; Cao, D. Energy Management Strategies of Connected HEVs and PHEVs: Recent Progress and Outlook. *Prog. Energy Combust. Sci.* **2019**, *73*, 235–256. [CrossRef]
11. Zhang, C.; Vahidi, A.; Pisu, P.; Li, X.; Tennant, K. Role of Terrain Preview in Energy Management of Hybrid Electric Vehicles. *IEEE Trans. Veh. Technol.* **2010**, *59*, 1139–1147. [CrossRef]
12. Zheng, C.; Xu, G.; Xu, K.; Pan, Z.; Liang, Q. An Energy Management Approach of Hybrid Vehicles Using Traffic Preview Information for Energy Saving. *Energy Convers. Manag.* **2015**, *105*, 462–470. [CrossRef]
13. Hofstetter, M.; Ackerl, M.; Hirz, M.; Kraus, H.; Karoshi, P.; Fabian, J. Sensor Range Sensitivity of Predictive Energy Management in Plug-in Hybrid Vehicles. In Proceedings of the 2015 IEEE Conference on Control Applications (CCA), Sydney, Australia, 21–23 September 2015; IEEE: Sydney, Australia, 2015; pp. 1925–1932.
14. Ubiergo, G.A.; Jin, W.-L. Mobility and Environment Improvement of Signalized Networks through Vehicle-to-Infrastructure (V2I) Communications. *Transp. Res. Part C Emerg. Technol.* **2016**, *68*, 70–82. [CrossRef]
15. Lai, L.; Ehsani, M. Dynamic Programming Optimized Constrained Engine on and off Control Strategy for Parallel HEV. In Proceedings of the 2013 IEEE Vehicle Power and Propulsion Conference (VPPC), Beijing, China, 15–18 October 2013; IEEE: Beijing, China, 2013; pp. 1–5.
16. Li, G.; Gorges, D. Fuel-Efficient Gear Shift and Power Split Strategy for Parallel HEVs Based on Heuristic Dynamic Programming and Neural Networks. *IEEE Trans. Veh. Technol.* **2019**, *68*, 9519–9528. [CrossRef]
17. Xiao, R.; Liu, B.; Shen, J.; Guo, N.; Yan, W.; Chen, Z. Comparisons of Energy Management Methods for a Parallel Plug-In Hybrid Electric Vehicle between the Convex Optimization and Dynamic Programming. *Appl. Sci.* **2018**, *8*, 218. [CrossRef]
18. Pei, D.; Leamy, M.J. Dynamic Programming-Informed Equivalent Cost Minimization Control Strategies for Hybrid-Electric Vehicles. *J. Dyn. Syst. Meas. Control* **2013**, *135*, 051013. [CrossRef]
19. Guo, L.; Gao, B.; Gao, Y.; Chen, H. Optimal Energy Management for HEVs in Eco-Driving Applications Using Bi-Level MPC. *IEEE Trans. Intell. Transp. Syst.* **2017**, *18*, 2153–2162. [CrossRef]
20. Heppeler, G.; Sonntag, M.; Wohlhaupter, U.; Sawodny, O. Predictive Planning of Optimal Velocity and State of Charge Trajectories for Hybrid Electric Vehicles. *Control Eng. Pract.* **2017**, *61*, 229–243. [CrossRef]
21. Qi, X.; Wu, G.; Hao, P.; Boriboonsomsin, K.; Barth, M.J. Integrated-Connected Eco-Driving System for PHEVs with Co-Optimization of Vehicle Dynamics and Powertrain Operations. *IEEE Trans. Intell. Veh.* **2017**, *2*, 2–13. [CrossRef]
22. Lee, G.; Ha, S.; Jung, J. Integrating Driving Hardware-in-the-Loop Simulator with Large-Scale VANET Simulator for Evaluation of Cooperative Eco-Driving System. *Electronics* **2020**, *9*, 1645. [CrossRef]
23. Lee, J.; Lee, H. A New HEV Power Distribution Algorithm Using Nonlinear Programming. *Appl. Sci.* **2022**, *12*, 12724. [CrossRef]

24. Natural Resource Canada, "Understanding the Tables". Available online: https://natural-resources.canada.ca/energy-efficiency/transportation-alternative-fuels/personal-vehicles/choosing-right-vehicle/buying-electric-vehicle/understanding-the-tables/21383 (accessed on 18 April 2023).
25. Deng, T.; Tang, P.; Luo, J. A Novel Real-time Energy Management Strategy for Plug-in Hybrid Electric Vehicles Based on Equivalence Factor Dynamic Optimization Method. *Int. J. Energy Res.* **2021**, *45*, 626–641. [CrossRef]
26. Hu, J.; Shao, Y.; Sun, Z.; Wang, M.; Bared, J.; Huang, P. Integrated Optimal Eco-Driving on Rolling Terrain for Hybrid Electric Vehicle with Vehicle-Infrastructure Communication. *Transp. Res. Part C Emerg. Technol.* **2016**, *68*, 228–244. [CrossRef]